Detection of the damage in concrete cover using ultrasound

B. PIWAKOWSKI [1], S. OULD-NAFFA [1], M. GOUEYGOU [1] and F. BUYLE-BODIN [2]

[1] *Ecole Centrale de Lille, France*
Bogdan.Piwakowski@ec-lille.fr

[2] *Laboratory of Mechanics*
Ecole Universitaire d'Ingénieurs de Lille
URA CNRS 1441, France

This paper deals with a non-destructive method for characterizing the degraded cover of concrete structures using high-frequency ultrasound (0.5 to 1 MHz). Although such a frequency range is unusual in civil engineering, it is well suited to the kind of defect to be detected, as it corresponds to a thin near-to-surface layer with increased porosity and density of microcracks.

This work has been carried out parallel in three directions: experimental ultrasonic characterization via the measurements of the acoustic speed and absorption as a function of the damage, research for an adequate signal processing suitable to access the extremely high absorption in degraded concrete cover and finally research of the correlation between the "ultrasound" parameters, and the "civil engineering parameters" like porosity or elastic modulus and the cube compressive strength – in order to perform the correct interpretation of the ultrasonic results. The velocity and attenuation measurements were made on both halves of a concrete slab. One half was immersed into an acid solution for 15 to 45 days, while the other half remained sound. These measurements were made for longitudinal, transverse and surface waves. The results obtained show a 23% decrease of ultrasonic pulse velocity and an increase of attenuation in the degraded material for a factor of 8 relative to the sound material.

The second subject of interest addresses the problem of evaluating the acoustic attenuation. The signals acquired from the highly attenuative and scattering medium are characterized by a poor signal-to-noise ratio. Therefore, an accurate estimate of attenuation cannot be obtained from a single measurement, but multiple measurements must be combined. The "cross spectrum" method, based on a system identification approach is used.

The transition between the acoustic and civil engineering domains is obtained by measuring of the porosity of the degraded sample and correlating it with the elastic modulus and the acoustic velocity and absorption.

1. Introduction

Concrete cover degradation is induced by aggressive agents in the ambiance, such as humidity, chemicals or temperature variations [Torrenti et al., 1999]. At an early stage, it manifests itself as a thin layer with higher porosity and higher density of microcracks compared with sound concrete. Later, the growth of the degraded layer into the heart of the structure may cause larger cracks, thus decreasing significantly the concrete strength. Therefore, the on-site non destructive evaluation of concrete cover is vital to monitor the integrity of concrete structures and prevent irreversible damage. Various methods are available today for testing concrete structures [Bungey and .Millard, 1986]. Among them, ultrasonic testing methods can be distinguished as they are non destructive and applicable on site. Low-frequency ultrasound (50 kHz) is routinely used to characterize large defects (a few cm large) at large depths inside the structure [Krause, et al, 1997]. However, such a frequency range is not suitable to the kind of defect to be detected in concrete cover. Our preliminary experiments [Ould-Naffa et al., 2001] have shown that the sensitivity of ultrasound parameters to cover degradation is higher when the wavelength becomes comparable to the thickness of the degraded layer, i.e. a few millimeters. Given the propagation velocity in concrete, ultrasonic waves with significant frequency components between 0.5 to 1 MHz are required to characterize concrete cover degradation with high sensitivity.

Our primary goal is to establish a correlation between acoustic parameters and the growth of the degraded layer. Secondly, we aim at determining the most sensitive evaluation method as regards to the wave type (LW, TW or SW) and the measured parameter (velocity or attenuation).

This work has been carried out in three parallel directions: experimental ultrasonic characterization via the measurements of the acoustic speed and absorption as a function of the damage, study of an adequate signal processing in order to access the extremely high absorption in degraded concrete cover and finally the research of the correlation between the porosity, the elastic modulus, the cube compressive strength and the acoustic quantities like velocity and absorption.

2. Experimental setup

2.1. Chemical degradation of the concrete cover

In order to make possible a systematic and "controlled" detection of the concrete cover degradation, the concrete samples were degraded chemically by immersing half of a concrete sample into an ammonium nitrate (NH_3NO_4)

solution with 437 g/l density, while the other half remained sound. The degradation procedure was carried out for periods of 15, 30 and 45 days. Such procedure is commonly used to accelerate concrete degradation [Torrenti et al.,1999]. The symbolic scheme of the degradation tank and the photograph of the section of the degraded mortar sample are shown in Fig. 1. The depth of the degradation and the global porosity of the degraded sample were measured after each degradation period. The porosity of the degraded layer was then estimated. As shown Fig. 2, the obtained global porosity and the depth of the degraded layer increase as the function of the time of degradation, whereas the porosity of the degraded part maintains constant at 24%.
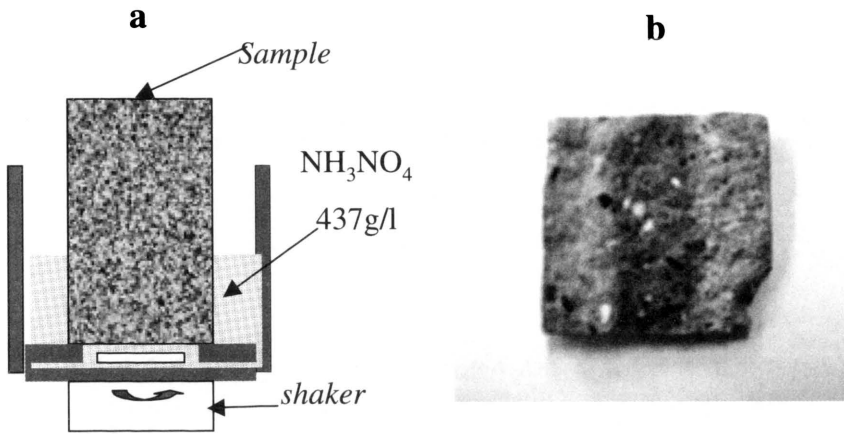

FIGURE 1. (a) Chemical degradation setup. (b) Sample of chemically degrades mortar.
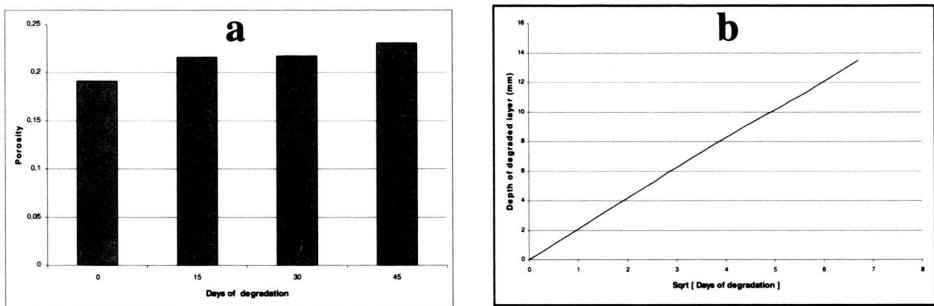

FIGURE 2. Effects of the degradation. (a) Global porosity as a function of time of degradation. (b) Depth of the degraded layer as a function of the square root of the time of degradation.

At the end of each period of the degradation, the acoustic velocity and attenuation were also measured and compared on both halves of the sample. Three types of elastic waves were concerned in these measurements: longitudinal (LW), transverse (TW) and surface waves (SW).

The studied sample of concrete slab is shown in Fig. 3a. Its dimensions were chosen to avoid edge effects in the wave propagation and allow transmission of ultrasound, and possibly multiple reflections, between both sides of the slab. The measurements were performed on a mortar (in order to limit the heterogeneity of the material, no gravel were added) and then on a concrete (with gravel). The composition of the studied samples is given in Table 1.

TABLE 1. Composition of the samples.

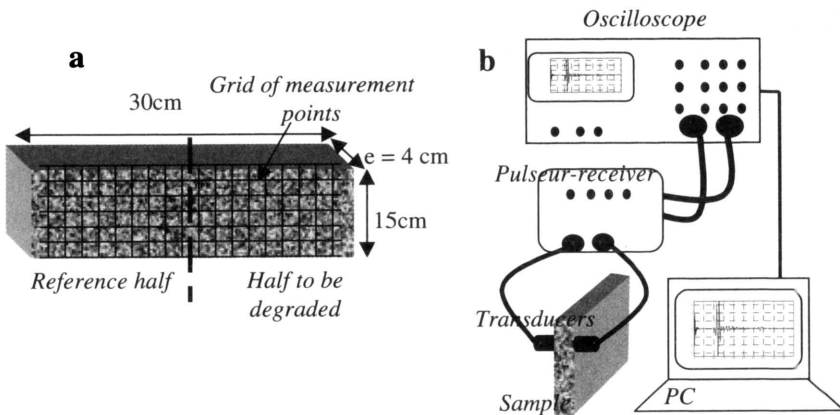|	Water	Cement	Gravel	Sand 0.5 mm
Mortar	11	22	0	67
Concrete	7	14	43	36

FIGURE 3. (a) Sample of mortar (concrete) used for the experiments. (b) Measurement setup.

2.2. Measurements of acoustic parameters

The measurement setup is shown in Fig. 3b. It includes a pulser-receiver (Sofranel 5055PR), a pair of contact transducers (Panametrics), a digital oscilloscope and a personal computer. The parameters of the transmit and

receive transducers are given in Table 2. Transducers were coupled to the sample using SWC gel (Sofranel). To generate surface waves, a LW transducer was coupled with a wedge of Teflon. The wedge angle was set to the critical angle of refraction for the transverse wave in concrete. Acoustic parameters (velocity and attenuation) were measured using through transmit mode. Although mortar is much more homogeneous than concrete with grains, the measured acoustic parameters were found to vary significantly across the sample surface. This is due to the presence of larger sand grains (up to 2 mm large) and to the lack of repetitivity in coupling the transducer to the sample. Therefore, transmission measurements were made on a grid of 72 points (36 points on each half, see Fig. 3). The results are presented as distributions or histograms, along with average values.

TABLE 2. Composition of the samples.

Type of wave	Resonant frequency [MHz]	Diameter [mm]
Longitudinal (T and R)	1	15
Transversal (T and R)	0.5	29
Surface – reception	5	5
Surface – emission	1	15+(teflon wedge)

2.3. Determination of acoustic velocity and attenuation

The ultrasonic group velocity was measured using the most common mean i.e. directly from the time of flight Δt between the trigger signal corresponding to the pulse emission and the first received signal, as shown in Fig. 4.

Ultrasonic attenuation seems to be a relevant parameter for degraded material characterization. There are various setups to acquire signals for measuring attenuation [Bamber, 1997] and different methods for quantitatively estimating the attenuation coefficient [Kuc, 1984].

In our case the correct evaluation the acoustic attenuation in degraded samples displays a special problem and requires special interest [Goueygou et al., 2001]. In the general case, the attenuation coefficient $\alpha(f)$ is measured as a function of frequency from the direct comparison of the spectra $S_1(z, f)$ and $S_2(z, f)$ of the transmitted signal $s_1(z_1, t)$ and its second multiple reflection $s_2(z_2, t)$ (see Fig. 4):

$$\alpha(f) = \frac{1}{z_2 - z_1} \left[20 \log_{10} \left(\frac{S_1(f)}{S_2(f)} \right) - 20 \log_{10} \left(\frac{z_2}{z_1} \right) \right]. \qquad (2.1a)$$
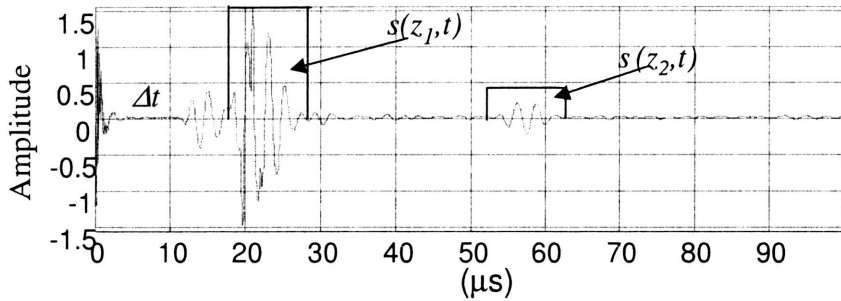
FIGURE 4. Example of the direct signal transmitted through the sample and its second multiple reflection.

Since signals acquired from the highly attenuative, inhomogenous and scattering medium are characterized by a poor signal-to-noise ratio and high dispersion, an accurate estimate of attenuation cannot be obtained from a single measurement, but multiple measurements must be combined. Since the spectra $S(z, f)$ are limited in frequency domain, the values of the obtained absorption as a function of the frequency is valid only in this frequency region where the signal to noise ratio is sufficiently high. In order to access the region of the validity for α the "cross spectrum" method, based on a frequency-domain identification technique is used [Bendat, 1986]. The mean estimate $G_{s_1 s_2}(f)$ over n measurements of the cross spectrum of signals $s_1(t)$ and $s_2(t)$, and the mean estimate $G_{s_1 s_1}(f)$ of the autospectrum of n signals $s_1(t)$ are computed $n = 36$ is the number of the measurement points). Finally the absorption coefficient, (expressed in dB/m) is found from the following formula:

$$\alpha(f) = \frac{1}{z_2 - z_1} \left\{ 20 \log_{10} \left[\frac{|G_{s_1 s_2}(z_1, z_2, f)|}{|G_{s_1 s_1}(z_1, f)|} \right] \right.$$

$$\left. - 20 \log_{10} \operatorname{corr}(z_1, z_2, f) \right\}, \quad (2.1b)$$

which replaces here the classical solution given by means of Eq. (2.1a). The $\operatorname{corr}(z_1, z_2, f)$ is a factor for correcting diffraction effects which was computed numerically [Xu and Kaufman, 1993]. The signals $s(z_1, t)$ and $s(z_2, t)$ are extracted from the recorded data by windowing.

The region of the validity for $\alpha(f)$ is found from the the coherence function γ between variables $s_2(t)$ and $s_1(t)$ computed as:

$$\hat{\gamma}_{1 \to 2}(f) = \frac{|G_{s_1 s_2}(f)|}{\sqrt{G_{s_1 s_1}(f) G_{s_2 s_2}(f)}}. \quad (2.2)$$

3. Experimental acoustic characterisation of the damaged concrete cover

Figure 5 presents the measured velocity distributions on the degraded half and on the sound half of the sample for 15, 30 and 45 days of degradation. A significant decrease of the average velocity with the time of degradation is observed. It is highlighted by the increasing distance between the peaks of the histograms corresponding to the degraded and to the sound material. Degradation, though, doesn't seem to have any effect on the variance of the measured velocity. The evolution of the measured velocity with degradation is summarized in Fig. 5d, showing the shift of velocity Δv relative to the value v_o obtained on the sound half. Notice that the greatest variation is observed for the surface wave. It rises up to 24% after 45 days. However, the decrease of SW velocity tends to slow down for longer degradation times. This may be explained by the fact that the SW propagates within a depth of the order of one wavelength. As the thickness of the degraded layer increases and goes beyond the depth of propagation of the SW, the SW tends to "sense" only one kind of material with identical properties.
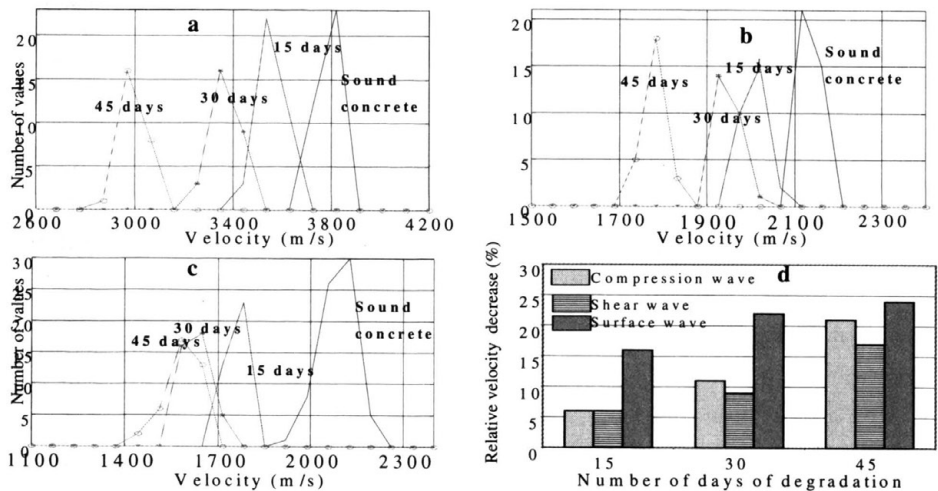

FIGURE 5. The velocity histograms distributions for the sound mortar and after 15, 30 and 45 days of degradation. (a) longitudinal waves; (b) transverse waves; (c) surface waves; (d) the summary of the results.

Figure 6 compares the results obtained for the mortar and concrete for the case of 30 days of degradation. It is observed that, as it might be expected, the dispersion of the results increases for the concrete and that the velocity
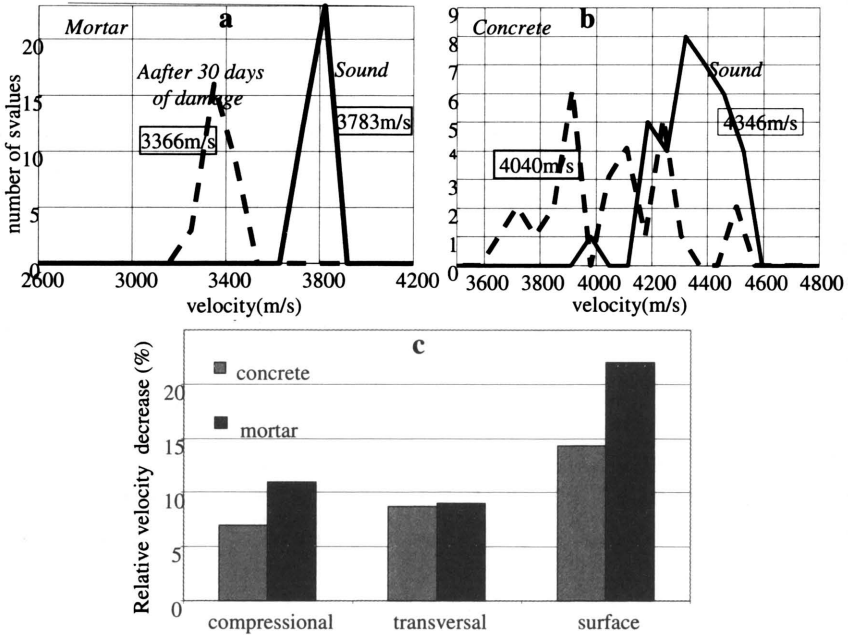
FIGURE 6. Comparison of the mortar with the concrete. (a), (b) The velocity histograms distributions for the sound sample and mortar and after 30 days of degradation. (c) Summary of results obtained for longitudinal, transverse and surface waves.

shift caused by the degradation is relatively smaller than that obtained for the mortar. This observation might be explained by the fact that gravel is less degraded than cement, so the degraded volume becomes smaller for concrete.

Figure 7 shows the attenuation coefficients obtained using to the procedure described in Sec. 1. The region of validity of the results (indicated by an ellipse) corresponds to the area where the coherence function γ reaches maximum values, close to unity. We observe that the obtained plots of $\alpha(f)$ fit the straight line: $\alpha(f) = \alpha_o f$, thus indicating a dramatic rise of the absorption expressed in terms of α_o [dB/(m MHz)] as a function of the time of degradation.

Figure 7d summarizes the increase of attenuation – relative to the attenuation of the sound half of the sample – versus time of degradation. Attenuation values are given at frequencies corresponding to the maximum energy of the wave propagating in the sample. As it may be seen in the plots of coherence function γ, the absorption causes the shift of the spectrum towards lower frequencies. Those frequencies are different for each type of wave, as the transducer used to generate those waves has different central frequen-
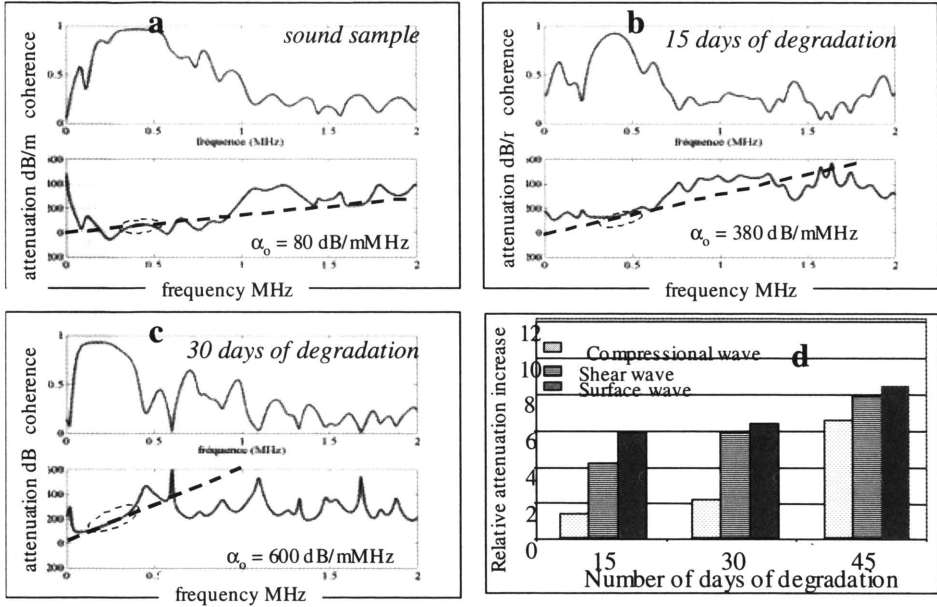
FIGURE 7. (a), (b), (c) Examples of attenuation α and of the associated coherence function γ as a function of frequency, obtained for the transversal waves. (d) Summary of results obtained for longitudinal, transverse and surface waves showing the relative increase of the attenuation coefficient as a function of the degradation time.

cies (generally the results fit in the range 0.2-0.6 MHz). The obtained results show a dramatic increase of attenuation with the time of degradation. This increase is especially pronounced for the surface wave, where it raises up to 8 times after 45 days of degradation

4. Assessment of the mechanical parameters from acoustic measurements

The Young modulus E, the dynamic modulus K and the Poisson coefficient ν may be found using well-known formulae:

$$E = \rho c_T^2 \frac{3c_L^2 - 4c_T^2}{c_L^2 - c_T^2}, \qquad \nu = \frac{c_L^2 - 2c_T^2}{2(c_L^2 - c_T^2)}, \qquad K = \rho \left(c_L^2 - \frac{4}{3} c_T^2 \right). \qquad (4.1)$$

The Poisson coefficient $\nu = 0.26$ and the density $\rho = 2465 \, \mathrm{kg/m^3}$ are found to be constant with the time of degradation. The parameters E and K computed from the velocity data [Eq. (4.1)] are shown in Fig. 8a.
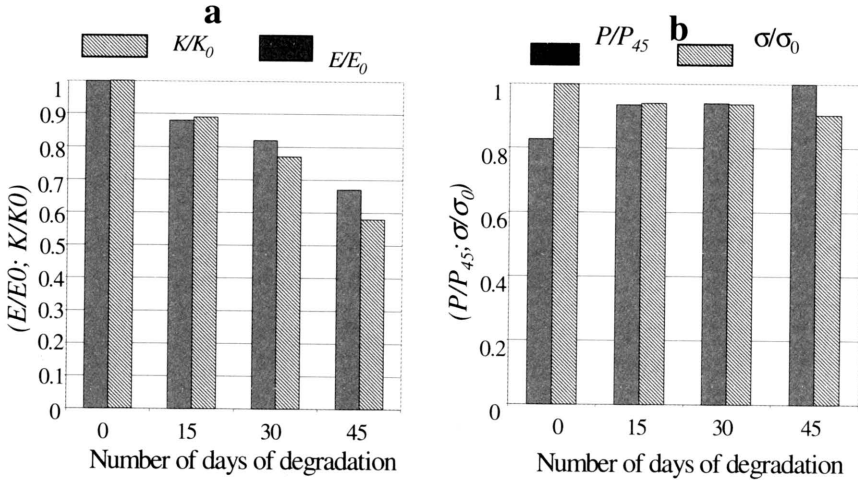
FIGURE 8. (a) Normalized elastic modulus E and K as a function of the degradation time. (b) Normalized global porosity P and associated normalized compressive strength σ as a function of the degradation time.

Similarly, the measurements of porosity reported in Sec. 1 enables us to estimate the compressive strength of the cube, using the well known Feret formula [Carde, 1986]:

$$\sigma = \sigma_o (1 - P)^2, \qquad (4.2)$$

where p indicates the porosity (in %) and σ_o is the compressive strength of the porosity-free sample. Figure 8b summarizes the relative decrease of σ and increase of P as a function of the time of degradation.

Finally, correlating the time of degradation and the obtained acoustic velocities (see Sec. 2) the relative drop of the Young modulus and the relative drop of the compressive strength as a function of the time of degradation may be found. These plots are shown in Fig. 9.
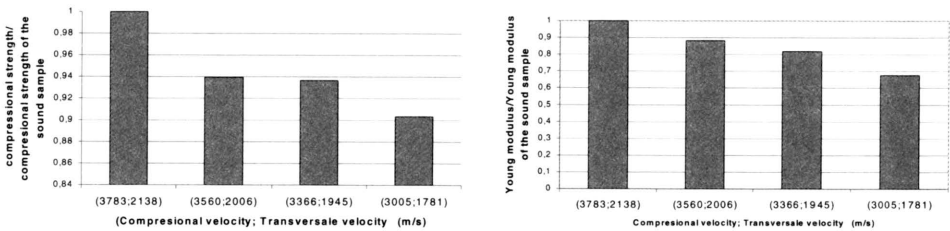

FIGURE 9. (a) Normalized elastic modulus E as a function of acoustic velocity, (b) Normalized compressive strength as a function of acoustic velocity.

5. Conclusions

The effect of degradation on the acoustic parameters of mortar was evidenced for all three types of waves. As expected, a decrease of velocity and an increase of attenuation were observed. Similar trends were observed with heterogeneous concrete, but the variance of the results made their interpretation difficult. In the case of mortar, velocity decrease achieved 24% for the surface wave, whereas attenuation increased dramatically up by a factor of 8 for the transverse wave. The high-frequency ultrasonic wave is thus able to detect changes in the micro-structure of the cover at an early stage (15 days). Our results highlight that attenuation is extremely sensitive to the degradation. Furthermore, preliminary experiments (not shown here) using much lower frequency (50 kHz transducers) have shown that there was no measurable attenuation difference at such a frequency range between the degraded and the sound material. This confirms that our choice of relatively higher frequency is relevant to sense the small thickness of the degraded layer.

Among the three types of elastic waves, the surface wave seems to be the most appealing for concrete cover evaluation. First, it was found to be highly sensitive to cover degradation. Second, its depth of penetration is frequency-dependent. This property may be useful to inspect the concrete cover at different depths and thus to estimate the thickness of the degraded layer. Third, it is well suited to on-site inspection as it requires access to one side of the structure only. Further studies will concentrate on using surface waves as a means to test and characterize concrete cover.

In parallel the problem of evaluating the acoustic attenuation in highly attenuative and scattering medium is approached. Since an accurate estimate of attenuation cannot be obtained from a single measurement, multiple measurements must be combined. The "cross spectrum" method, based on a system identification approach was used. Except the signal to noise ratio improvement, its advantage is that a coherence function may be computed, in order to define a valid frequency range for the attenuation estimate. This characteristic is of great importance because the measured values are a priori unknown. Consequently, the cross spectrum approach method seems to be suitable for evaluating attenuation in "difficult" materials, such as concrete.

References

1. J.C. BAMBER, Acoustical characteristics of biological media, in: M.J. Crocker (Ed.) *Encyclopedia of Acoustics*, pp.1703-1725, John Wiley & Sons, New York, 1997.

2. J.S. BENDAT and A.G. PIERSOL, *Random Data : Analysis and Measurement Procedure*, John Wiley & Sons, New York, 1986.

3. J.H. BUNGEY and S.G. MILLARD, *Testing of Concrete in Structures*, Blackie Academoic & Professional, Glasgow 1996.

4. *C. Carde, Caractérisation et modélisation de l'altération des propriétés mécaniques due a la lixiviation des matériaux cimentaires*, Thèse de doctorat INSA 1996.

5. M. GOUEYGOU, B. PIWAKOWSKI, S. OULD NAFFA and F. BUYLE-BODIN, Assessment of broadband ultrasonic attenuation measurements in inhomogenous media, *Ultrasonics International 2001*, Delft, July 2-5, 2001.

6. M. KRAUSE et al., Comparison of pulse-echo methods for testing concrete, *NDT&E International*, Vol.30, No.4, pp.195-204, 1997.

7. R. KUC, Estimating acoustic attenuation from reflected ultrasound signals: comparison of spectral-shift and spectral-difference approach, *IEEE ASSP Transactions*, Vol.32, No.1, pp.1-6, 1984.

8. S. OULD-NAFFA, M. GOUEYGOU, B. PIWAKOWSKI and F. BUYLE-BODIN, Detection of chemical damage in concrete using ultrasound, *Ultrasonics International 2001*, Delft, the Netherlands, July 2001.

9. J.-M. TORRENTI, O. DIDRY, J.-P. OLLIVIER and F. PLAS, *La dégradation des bétons*, Hermes, Paris 1999.

10. W. XU, J.J. KAUFMAN, Diffraction correction methods for insertion ultrasound attenuation estimation, *IEEE Transactions on Biomedical Engineering*, Vol.40, No.6, pp.563-570, 1993.

———◇———